INTER-AMERICAN TROPICAL TUNA COMMISSION

***AD-HOC* PERMANENT WORKING GROUP ON FADS**

6TH MEETING

(by videoconference)
12-13 May 2022

DOCUMENT FAD-06-03

TROPICAL TUNA BIOMASS INDICATORS FROM ECHOSOUNDER BUOYS IN THE EASTERN PACIFIC OCEAN

Jon Uranga[1], Jon Lopez[2], Maitane Grande[1], Cleridy E. Lennert-Cody[2], Iñaki Quincoces[1], Igor Granado[1], Mark N. Maunder[2], Alexandre Aires-da-Silva[2], Gorka Merino[1], Hilario Murua[3], Josu Santiago[1]

SUMMARY

The collaboration with some tropical tuna vessel-owners associations operating in the eastern Pacific Ocean and the buoy-providers, allowed access to information recorded by their satellite-linked GPS tracking echosounder buoys since 2010. These instrumented buoys inform fishers remotely in real-time about the accurate geolocation of the fish aggregating devices (FAD) and the presence and abundance of fish aggregations underneath them. Therefore, echosounder buoys are considered good observation platforms to provide catch-independent data and potentially evaluate abundances of tunas and accompanying species at FADs. Current echosounder buoys provide a single biomass value without discriminating species or size composition of the fish. Therefore, the echosounder buoy data has to be combined with fishery data, species composition and average size, to obtain specific species indicators. This paper presents a novel method and an estimation of an index of abundance for skipjack tuna in the eastern Pacific Ocean derived from echosounder buoys for the period 2012-2021, which is used in the interim stock assessment.

1. INTRODUCTION

Historically, stock assessments for tropical tuna species have relied almost exclusively abundance estimators that are dependent on commercial catches and fishing effort derived from captain's logbooks or observer data (Maunder and Punt 2004). These catch and effort data are used to provide information on relative trends in fish abundance that are integrated in fish stock assessment models to assess the state and the evolution of fish stocks (Quinn and Deriso 1999). Relative abundance indices based on Catch-Per-Unit-Effort (CPUE) are related with the abundance, through the catchability coefficient (q). However, this proportionality is affected by various factors, such as variations in fishing efficiency, spatial dynamics of the fleet or species, and changes in target species (Maunder and Punt 2004; Maunder et al. 2006). To try to remove the effects of these factors on the CPUE data so that changes related to population abundance can be identified, standardization of CPUE is used.

In the case of the tropical tuna purse-seine fishery, fishing efficiency has significantly increased with the incorporation of new technology on board and with the use of Fish Aggregating Devices (FADs) (Lopez et al. 2014; Torres-Irineo et al. 2014; Gaertner et al. 2016). The difficulties of providing new

[1] AZTI, Marine Research, Basque Research and Technology Alliance (BRTA). Txatxarramendi ugartea z/g, 48395. Sukarrieta - Bizkaia, Spain

[2] Inter-American Tropical Tuna Commission, 8901 La Jolla Shores Drive, La Jolla CA 92037, USA

[3] International Seafood Sustainability Foundation (ISSF).1440 G Street NW Washington DC 20005.U.S. hmurua@iss-foundation.org

covariates based on fine-scale data to reflect these technological changes and effort creep and the lack of a good proxy for purse-seine effort, and in particular on FADs, hampered scientists from standardizing the FAD fishing CPUEs (Gaertner et al. 2016; Katara 2018; Wain 2021). Consequently, the purse-seine FAD CPUE has not been included in tropical tuna stock assessment models. At the same time, successful science-industry collaborative projects have started to provide information on the adoption of technological advances in this fleet as a mean to improve the CPUE standardization process (Wain 2021) and ultimately, tropical tuna assessments.

The introduction of the satellite-linked echosounder buoys attached to those FADs (Scott 2014) provides an alternative method to observe the dynamics of aggregations and allow for estimation of indices that are catch-independent. These instrumented buoys provide fishers daily information on buoy position and a rough estimate of the fish biomass underneath the FADs and makes them effective observation platforms for monitoring tuna and other species aggregations remotely in a systematic non-invasive way. In recent years, industry-research collaborations have allowed collection of buoy-derived data, and scientific methodological frameworks have been developed to extract reliable information from these data (Orúe et al., 2019). This information has proven to be useful for science and has already been used to, for example, investigate tuna behaviour and ecology around FADs and provide buoy-derived abundance indices (Lopez et al. 2014; Capello et al. 2016; Moreno 2016; Orúe et al., 2019; Santiago et al. 2019; Baidai 2020).

Also recently, the Buoy-derived Abundance Index (BAI), which is based on the proportional relationship between the echosounder buoy biomass estimate and the total abundance of tuna, has been incorporated in ICCAT yellowfin and bigeye stock assessments (ICCAT 2019, 2021). Building on that success, a framework of collaborative work was stablished, with the support of the International Seafood Sustainability Foundation (ISSF), between the Inter-American Tropical Tuna Commission (IATTC) and AZTI, in collaboration with echosounder buoy providers and some tropical tuna purse seiner fishing companies operating in the eastern Pacific Ocean (i.e., companies integrated in the fishing vessel association OPAGAC-AGAC and Cape Fisheries). This collaboration aims to produce reliable BAI for tropical tuna species in the region. This paper presents the application of this novel method to generate an index of abundance for skipjack tuna in the EPO derived from echosounder buoy information for the period 2012-2021, which has been included in the interim skipjack assessment conducted by the IATTC staff in 2022 (SAC-13-07) and can inform future abundance indices for all three of the major tropical tuna species (skipjack, yellowfin and bigeye tuna). Some preliminary results of the collaborative project were presented at the 5th meeting of the *Ad-hoc* Permanent Working Group on FADs, along with a list of ideas and tasks to further improve these indicators. This document updates the results of the previous index and presents the progress made in with certain aspects of the methodology during 2021 and 2022.

2. MATERIAL AND METHODS

2.1 Acoustic data pre-filtering

The main data used in this analysis is recorded by satellite linked echo-sounder buoys attached to FADs used by the EPO tropical tuna purse-seine fishery. In this particular analysis, only data provided by the buoy manufacturer Satlink were used. The buoy technical specifications, per model, are shown in Table 1. All buoys record information from 3 to 115 m depth divided into 10 homogeneous vertical layers, each with a resolution of 11.2 m (the first 3 m correspond to the blind zone). During the period analyzed, January 2012 to December 2021, five different buoy models were used by the fleet: DS+, DSL, ISD, ISL and SLX (Table 1).

The fishing companies that kindly provided the information collected by their echosounder buoys were: Albacora, Calvo, Garavilla, Ugavi, and Cape Fisheries. This corresponds to a total of 23 purse-seine vessels from 5 different flags (Panama, Spain, Ecuador, El Salvador, USA) operating in the IATTC convention area.

A total number of 12.39 million acoustic records from 38,321 individual buoys were included in the database. Years 2010 and 2011 were discarded due to the low number of records available (Figure 1) and acoustic records from areas with low number of observations (less than 200 records in 5^{o}x5^{o} statistical rectangles) and those west of 150^{o}W were excluded for this analysis.

From each single data record, transmitted via satellite, the following information was extracted: "*Name*", unique identification number of the buoy, given by the model code (DS+, DSL, ISL, ISD, SLX) followed by 5-6 digits; "*OwnerName*", name of the buoy owner assigned to a unique purse-seine vessel; "*MD*", message descriptor (160, 161 and 162 for position data, without echosounder data, and 163, 168, 169 and 174 for echosounder data); "*StoredTime*", date (dd/mm/yyyy) and hour (HH:MM) of the position and the echosounder records; "*Latitude, Longitude*", record-associated GPS latitude and longitude information (in decimals); "*Bat*", battery charge level of the buoy, as a percentage (not provided, except for the D+ and DS+ models, in voltage); "*Speed*", estimated speed of the buoy in knots; "*Layer1-Layer10*", estimated tons of tuna by layer (values are estimated by a manufacturer´s method which converts raw acoustic backscatter into biomass in tons, using a depth layer echo-integration procedure based exclusively on an algorithm using the target strength (TS) and weight of skipjack tuna); "*Sum*", sum of the biomass estimated for all layers; "*Max*", maximum biomass estimated at any layer; and "*Mag1, Mag3, Mag5 and Mag7*", magnitudes corresponding to the counts of detected targets according to the TS of the detection peak.

A set of five filters were applied to the original data to remove artifacts: 1) isolated, duplicated and ubiquitous rows, that are mainly caused by satellite communication incidents; 2) buoys located 1 km or closer to land or located in the continental shelf (i.e., a bottom depth shallower than 200 m), detected and removed using shoreline data from the GSHHG database (Wessel 1996) and a worldwide global bathymetry information (Amante and Eakins 2009); and 3) "on-board" or "at sea" positions, identified using a Random Forest algorithm (Orue et al. 2019; Santiago et al. 2020), these cases are mainly related to buoy activations onboard vessels prior deployment and post retrieval.

In addition to the previously mentioned data cleaning filters, the following selection criteria (Santiago et al. 2020) were used to build the final dataset to feed into the standardization analysis: i) shallower layers (<25m) were excluded because they are consider to potentially reflect non-tuna species (e.g., Orue et al. 2019); ii) only data recorded around sunrise, between 4 a.m. and 8 a.m. in local time, were considered for the analysis because they are supposed to better capture the biomass under the FADs (e.g., Moreno et al. 2007 and FAD-06-01 – the hours around sunrise are fishers preferred setting times on FADs); and finally, iii) acoustic data belonging to what we defined as "virgin segments" were selected in order to use the segment of a buoy trajectory whose associated FAD likely represents a new deployment which has been potentially colonized by tuna and not fished yet. To calculate virgin segments, single buoy information was divided into smaller segments where the difference between two consecutive observations of the same buoy was larger than 30 days. Values of 5 and 15 days were also tested. The former seems unlikely since it may represent buoys that have been re-deployed at a fairly reasonable rate, whereas the later had no impact in the final indices. The segments with less than 30 observations and those having a time difference between any of the consecutive observations longer than 4 days during the first 35 days were removed. Finally, from the remaining data, we focused on the information corresponding to 20-35 days at sea, the time at sea for which FADs seem to be colonized (Orue et al. 2019). Figure 2 shows a diagram with an example of "virgin" segments used for the calculation of the BAI index.

2.2 From acoustic data to a species-specific abundance indicator

To calculate the biomass aggregated under a FAD from the acoustic signal, Satlink uses the Target Strength (TS) of one species, skipjack, to provide the biomass in tons, and thus, biomass data from Satlink has to be converted to decibels (acoustic information) reversing their formula for the biomass computation. Once the raw acoustic information is available, this can be recomputed into biomass

per species using standard acoustic abundance estimation equations (Simmons and MacLennan 2005):

$$Biomass_i = \frac{s_V \cdot Vol \cdot p_i}{\sum_i \sigma_i \cdot p_i}$$

where s_v is the volume backscattering strength, *Vol* is the sampled volume of the beam and p_i and σ_i are the proportion and linearized target strength of each species *i* respectively.

Species proportions in weight at 1°x1° and month resolution were extracted from logbooks (for class 1-5 vessels, ≤ 363 mt) and observers data (for class 6 vessels, >363mt) for 14 flags. Mean fish lengths (L_i), for 5°x5° area - month resolution were obtained from IATTC port-sampling data for skipjack (SKJ), bigeye (BET) and yellowfin (YFT), which were raised to the catch in the sampled wells. Weights were estimated using IATTC weight-length conversion factors. Then, the following Target Strength-length relationships were used to obtain linearized TS per kilogram:

$$\sigma_i = \frac{10^{(TS)/10}}{w_i}$$

where w_i is the mean weight of each species and TS is the backscattering cross-section of each species individual fish. The linear value of TS is assumed to be proportional to the square of the fish length (Simmons and MacLennan 2005).

$$TS = 20log(Li) + b20$$

Given that each brand uses different operating frequencies, we used different b20 values for each species (b20 is the so-called reduced target strength). For Satlink, the b20 values were obtained from Boyra et al. (2018) for SKJ, from Bertrand and Josse (2000) and Oshima (2008) for YFT, and from Boyra et al. (2018) for BET.

Since information on catch composition for the same time-area strata are not always available for acoustic records, we followed a three-step hierarchical process to get this information: 1) use the species distribution data from the same 5°x5° grid, year and month; 2) alternatively, use the same quarter and 5°x5° grid; and finally, as a last option, 3) use the mean values of species distribution data at a quarter and region resolution, shown in Figure 3.

The results presented in this document correspond to the fraction of the acoustic signal estimated to be informative for the biomass of skipjack.

2.3 The BAI index: Buoy-derived Abundance Index

The estimator of abundance, BAI, was defined as the 0.9 quantile of the integrated acoustic energy observations in each of the "virgin" sequences. A high quantile was chosen because the large values are likely produced by tuna (opposite of what is expected for other species). This assumption is also made by all the buoy manufacturers in the market, which use the maximum value as the summary of biomass for each time interval. In our case, a high quantile was selected rather than the maximum to try to provide a more robust estimator by avoiding outlier values. The total number of “virgin” sequences analyzed, and hence the number of observations include in the model, is 14,121, of which 14,068 (99.62%) had positive values.

2.4 The model

The covariates used in the standardization process and fitted as categorical variables were year-quarter, 5x5º area and buoy model. A proxy of 1ºx1º and monthly FAD densities (average number of unique buoys over each month in a 1ºx1º area) and the following environmental variables were included as continuous variables in the model:

- Ocean mixed layer thickness: defined as the thickness of the thermocline in the point of density increase, compared to density at 10 m depth, corresponds to a temperature decrease of 0.2°C in local surface conditions (θ10m, S10m, P0= 0 db, surface pressure).
- Chlorophyll: Mass concentration of chlorophyll a in sea water at the sea surface (in mg/m^3).
- Sea Surface Temperature (SST): Ocean Sea Surface temperature (in C).
- SST and Chlorophyll fronts: Oceanographic front detection was performed using the "*grec*" package in R (Team 2013) for each daily SST and CL datasets, which provides algorithms for detections of spatial patterns from oceanographic data using image processing methods based on Gradient Recognition (Belkin and O'Reilly 2009).

  The model we propose is based on an assumption very similar to the fundamental relationship between CPUE and abundance widely used in quantitative fisheries analysis. In our case, the signal from the echosounder is assumed to be proportional to the abundance of fish under the FAD:

$$BAI_t = \varphi \, . B_t$$

where BAI_t is the Buoy-derived Abundance Index and B_t is the abundance in time t (Santiago et al., 2016).

Although it would appear to be obvious, there is not a lot of literature available on the relationship between acoustic indicators and fishing performance. In general, it is assumed that acoustic echo-integration is a linear process, i.e., proportional to the number of targets (Simmons and MacLennan 2005) and has been experimentally proven to be correct with some limitations (Foote, 1983; Røttingen, 1976). Therefore, acoustic data (echo-integration) are commonly taken as a proxy for abundance and are used to obtain acoustic estimates of abundance for many pelagic species (Hampton 1996; ICES 2015; Masse et al. 2018).

As with catchability, the coefficient of proportionality ϕ is not constant for many reasons. In order to ensure that ϕ can be assumed to be constant (i.e., to control the effects other than those caused by changes in the abundance of the population) a standardization analysis should be performed by aiming to remove factors other than changes in abundance of the population. This can be performed standardizing nominal measurements of the echosounder using a Generalized Linear Mixed Modelling (GLMM) approach.

Because of the low proportion of zeros in the dataset (0.38%), they were excluded from the analysis and therefore the delta lognormal approach (Lo et al. 1992) was not considered. A GLMM with a log-normal error structured model was applied to standardize the non-zero acoustic observations. A stepwise procedure was used to fit the model with all the explanatory variables and interactions in order to determine those that significantly contributed to explaining the variability in the data. For this, deviance analysis and summary tables were created, and the final selection of explanatory variables was conducted using: a) the relative percent increase in deviance explained when the variable was included in the model (variables that explained more than 5% were selected), and b) The Chi-square ($\chi 2$) significance test.

Interactions between the temporal component (year-quarter) with the rest of the variables were also

evaluated. If an interaction was statically significant, it was then considered as a random interaction(s) within the final model (Maunder and Punt 2004).

The selection of the final model was based on the Akaike's Information Criterion (AIC), the Bayesian Information Criterion (BIC), and a Chi-square ($\chi 2$) test of the difference between the log- likelihood statistic of different model formulations. The year-quarter effect least square means (LSmeans) were bias corrected for the logarithm transformation algorithms using the approach described in Lo et al. 1992. All analyses were done using the lme4 package in R (Bates et al. 2014).

3. RESULTS

A total of 12.39 million acoustic records from 38,321 buoys for 2012-2021 were evaluated to create 14,121 observations for the GLMM analysis. Each observation was calculated as the 90% percentile of a "virgin" segment of buoy trajectories. A virgin segment represents a deployment that has been potentially colonized by tuna but not fished.

Figure 4 shows the histograms of the BAI and log transformed BAI nominal values. Log transformation makes the data to follow a normal distribution, as shown in the left panel of Figure 4. Figure 5 shows the spatial distribution [5°x5°] of the number of "virgin" segments of buoy trajectories that have been used in the GLMM analysis. The quarterly evolution of the number of observations on a 5°x5° grid is shown in Figure 6.

Figure 7 shows the quarterly evolution of the nominal log BAI index by squares of 5x5 degrees from 2012 to 2021.

The results of the deviance analysis are shown in Table 2. The model explained 37% of the total deviance. The most significant explanatory variables were year-quarter, 5°x5° area and the interaction year-quarter*area that was considered as random effect. No significant residual patterns were observed (Figure 8).

Quarterly series of standardized BAI index are provided in Table 2 and Figure 9. Three periods showed higher values: a) the beginning of the series, 2012, with wider confidence intervals due to the relatively low number of observations; b) the years 2015 and 2016; and c) the years 2019 and 2020. Apart from the first quarter from 2012 the CVs remain relatively stable during the whole time series at levels of 13-16%.

4. ADDITIONAL ANALYSES

This paper presents preliminary results on the abundance index for skipjack in the EPO following the methodology previously developed for tropical tuna stocks in other oceans (Santiago et al. 2019; Santiago et al. 2020a; Santiago et al. 2020b). This methodology is intended to be improved in the context of this collaboration based on the following aspects already identified as potential lines of investigation, some of them already initiated (Uranga et al., 2021):

a) Improve the determination of virgin segments: the current threshold of 30 days between two consecutive observations of the same buoy to consider trajectories of two different FADs may be too restrictive. A high threshold increases the certainty of differentiating new trajectories but directly impacts the number of observations available for analysis. Conversely, a low threshold of a few days increases the uncertainty in discriminating different trajectories, but also increases the number of observations.

As such, an exploratory study was carried out to analyze the possible effect of using different thresholds for virgin segment selection. As mentioned above, the objective of defining a threshold is to try to ensure that different trajectories from the same buoy correspond to different deployments or redeployments, and therefore, "new" FADs. The threshold also allows, within each trajectory, to

maximize the probability that the FAD has been colonized, while minimizing the probability that it has not been fished. Therefore, the assumption of 30 days is in some way conservative and implies the loss of potentially valuable data; but there is a gain in guaranteeing that the segments obtained actually correspond to different FADs. Conversely, assuming a gap of 5 days the number of observations substantially increases but at the risk of incorporating observations that may not really correspond to different FADs.

In order to assess the impact of the selection of this threshold, the index was re-estimated assuming 3 different values: 5, 15, and the original 30 days. The number of observations using more or less restrictive criteria was 14,121 (30 d), 19,532 (15 d) and 31,122(5 d). The resulting indices with the 15 day and 30 day assumptions provide fairly consistent results, but the trend is slightly different when a 5 day threshold is assumed (Figure 10).

b) Investigate whether the methodology of classification for virgin segments is accurate: Observer data and the data collected in the FAD forms by the fishing crew for unobserved trips can be used to help inform the virgin segment selection and the selection of the threshold of days between two consecutive observations of the same buoy. Both the observer data collection form and the FAD form were modified in 2019 to include specific fields for buoy identification. The quality and quantity of these data has been improving and future works could consider these data sources to investigate this matter in detail.

c) Improve the biomass colonization models: Currently, the virgin segment corresponds to 20-35 days since the estimated date of deployment of the FAD. According to Orue et al. (2019), who modelled the colonization processes at virgin FADs in the Indian Ocean using echosounder buoy data, tuna seem to arrive at FADs in 13.5±8.4 days, so we leave a period of 20 days since deployment to try to maximize the probability of the FAD being colonized. The period of observation was also limited to 35 days from deployment to minimize the probability of the FAD not being fished. Different time periods could be explored after modelling the different spatial-temporal patterns of FAD colonization processes in the EPO using a number of modelling approaches, from traditional GAMMs and GLMMs to most sophisticated machine learning algorithms like Boosted Regression Trees. Similarly, these models should also explore the influence of different factors in the colonization process to better understand its relationship with abundance at FADs.

d) Improve the statistical modelling: sensitivity tests will be performed to test the appropriateness of using normal and non-normal distributions. Moreover, the use of other metrics rather than the 90% percentile (mean, median, etc.) will be explored to better understand the effect of this selection in the final abundance index.

e) Improve the characterization of species composition for the strata of interest: different spatio-temporal strata or modeling approaches could be explored to characterize the species composition and sizes in the EPO. This could potentially affect the species-specific acoustic biomass estimations because these data are currently used to convert acoustic information into biomass. The three-step approach currently used with different time-area strata resolution could be reviewed and sensitivity analysis performed to test the robustness of the estimation to different assumptions.

In this sense, some exploratory analyses were conducted to explore the optimum size metric to be applied for the species-specific acoustic biomass estimations. Further sensitivity tests are needed but as a preliminary approach, the variability of four different size measures was explored (mean, median, mode and bimodal peaks). Pending further tests, differences between the four analyzed metrics are negligible (Figure 11) and thus, it should be expected that the effect of the different measures on the biomass estimate is minimal, and that the final BAI index would be insensitive to them.

f) Develop a methodology to predict species composition from acoustic samples: observer and logbook data on catch composition for individual sets could be analyzed using machine learning algorithms, where particular acoustic echograms would be related to specific species compositions. If successful, the methodology could move away from using spatio-temporal fishery statistics that rely on port-sampling and other data sources.

As a first step, the relationship between tuna catch composition recorded by observers and acoustic information at FADs was explored at the set level in the EPO for the period 2019-2021. A sensitivity test was conducted for three temporal windows for acoustic records (5, 15 and 30 days prior to the catch) and a number of metrics obtained from the acoustic data (Figure 12a): i) Unique biomass value of the cells above a certain threshold (maximum, 90% percentile, mean), ii) Sum of unique biomass values of the cells exceeding a certain threshold (maximum, 90% percentile, mean), iii) Buffers (1 cell around each candidate) are generated from those cells that exceed a certain threshold (maximum, 90% percentile, mean) and the biomass of these cells is summed, and iv) Maximum, mean, median, 99% percentile, 90% percentile and 75% percentile values for the whole temporal window.

Results of the sensitivity analysis showed that the means and 90th percentiles corresponding to the time frames closer to the fishing event (i.e., 5-15 days) seem to have the best performance (Figure 12b). As an example, Figure 13 shows the relationship between the 90th quantile of the entire 15-day window and its corresponding tuna catches, where the relationship is highly significant ($p<0.001$). However, this issue deserves further exploration and future efforts should be conducted to develop and validate the prediction models based in machine learning algorithms.

These issues reflected above are only examples of the improvement tasks that are being undertaken in the context of this collaborative joint project between AZTI and the IATTC staff, which benefits from the collaboration of the fleet, buoy providers and the ISSF. In this sense, the involvement of the industry, who kindly agreed to provide the historic data collected by their echosounder buoys, is instrumental to generate these valuable catch-independent indices of abundance. We deeply appreciate the involvement of OPAGAC and Cape Fisheries in this project and hope that other companies will join this initiative, retrieving historical information and committing to regularly provide this high-resolution buoy data beyond 2024 (i.e., Resolution C-21-04 request CPCs to provide raw echo-sounder buoy information during 2022-2024). In fact, this information and the advances in the associated scientific methodology can provide significant improvements to complement current stock assessments of tropical tuna stocks, providing indices that are less dependent on fisheries data and less affected by changes in fishing efficiency. The utility of this data is evident by its use in the interim skipjack stock assessment (SAC-13-07).

ACKNOWLEDGEMENTS

We want to express our gratitude to the following fishing companies that have provided acoustic information from their echosounder buoys: Albacora, Calvo, Garavilla, Ugavi and Cape Fisheries. And to the Basque Government and ISSF for funding this work.

REFERENCES

Amante, C. and B. Eakins (2009). "ETOPO1 1 arc-minute global relief model: procedures, data sources and analysis. NOAA Technical Memorandum NESDIS NGDC-24." National Geophysical Data Center, NOAA 10: V5C8276M.

Baidai, Y. D. A. (2020). Derivation of a direct abundance index for tropical tunas based on their associative behavior with floating objects, Université Montpellier.

Bates, D., M. Mächler, et al. (2014). "Fitting linear mixed-effects models using lme4." arXiv preprint arXiv:1406.5823.

Belkin, I. M. and J. E. O'Reilly (2009). "An algorithm for oceanic front detection in chlorophyll and SST satellite imagery." Journal of Marine Systems 78(3): 319-326.

Bertrand, A. and E. Josse (2000). "Tuna target-strength related to fish length and swimbladder volume." ICES Journal of Marine Science 57(4): 1143-1146.

Boyra, G., G. Moreno, et al. (2018). "Target strength of skipjack tuna (Katsuwanus pelamis) associated with fish aggregating devices (FADs)." ICES Journal of Marine Science 75(5): 1790-1802.

Capello, M., J. L. Deneubourg, et al. (2016). "Population assessment of tropical tuna based on their associative behavior around floating objects." Scientific Reports 6(1): 36415.

Gaertner, D., J. Ariz, et al. (2016). "Objectives and first results of the CECOFAD project." Collective Volume of Scientific Papers 72(2): 391-405.

Gaertner, D., S. Clermidy, et al. (2016). "Results achieved within the framework of the EU research project: Catch, Effort, and eCOsystem impacts of FAD-fishing (CECOFAD)." Acta Agriculturae Slovenica.

Hampton, I. (1996). "Acoustic and egg-production estimates of South African anchovy biomass over a decade: comparisons, accuracy, and utility." ICES Journal of Marine Science 53(2): 493-500.

ICCAT (2019). Report of the 2019 ICCAT yellowfin tuna stock assessment meeting., (Grand-Bassam, Cote d'Ivoire, 8-16 July 2019).

ICCAT (2021). Report of the 2021 ICCAT bigeye tuna stock assessment meeting., (Online, 19- 29 July 2021)

ICES (2015). Manual for International Pelagic Surveys (IPS). Series of ICES Survey Protocols. SISP 9 - IPS. 92 pp.

Katara, I., Gaertner, D., Marsac, F., Grande, M., Kaplan, D., Urtizberea, A., Abascal, F. (2018). Standardisation of yellowfin tuna CPUE for the EU purse seine fleet operating in the Indian Ocean. 20th session of the Working Party on Tropical Tuna.

Lo, N. C.-h., L. D. Jacobson, et al. (1992). "Indices of relative abundance from fish spotter data based on delta-lognornial models." Canadian journal of fisheries and aquatic sciences 49(12): 2515- 2526.

Lopez, J., G. Moreno, et al. (2014). "Evolution and current state of the technology of echo-sounder buoys used by Spanish tropical tuna purse seiners in the Atlantic, Indian and Pacific Oceans." Fisheries Research 155: 127-137.

Masse, J., A. Uriarte, et al. (2018). "Pelagic survey series for sardine and anchovy in ICES subareas 8 and 9—Towards an ecosystem approach." ICES cooperative research report(332).

Maunder, M. N. and A. E. Punt (2004). "Standardizing catch and effort data: a review of recent approaches." Fisheries Research 70(2-3): 141-159.

Maunder, M. N., J. R. Sibert, et al. (2006). "Interpreting catch per unit effort data to assess the status of individual stocks and communities." ICES Journal of Marine Science 63(8): 1373-1385.

Moreno, G., L. Dagorn, et al. (2007). "Fish behaviour from fishers' knowledge: the case study of tropical tuna around drifting fish aggregating devices (DFADs)." Canadian journal of fisheries and aquatic sciences 64(11): 1517-1528.

Moreno, G., Dagorn, L., Capello, M., Lopez, J., Filmalter, J., Forget, F., Sancristobal, I., . and Holland, K. (2016). "Fish aggregating devices (FADs) as scientific platforms." Fisheries Research 178: 122- 129.

Orue, B., J. Lopez, et al. (2019). "From fisheries to scientific data: A protocol to process information from fishers' echo-sounder buoys." Fisheries Research 215: 38-43.

Orue, B., J. Lopez, et al. (2019). "Aggregation process of drifting fish aggregating devices (DFADs) in the Western Indian Ocean: Who arrives first, tuna or non-tuna species?" PloS one 14(1): e0210435.

Orúe Montaner, B. (2019). "Ecology and behavior of tuna and non-tuna species at drifting fish aggregating devices (DFADs) in the Indian Ocean using fishers' echo-sounder buoys."

Oshima, T. (2008). "Target strength of Bigeye, Yellowfin and Skipjack measured by split beam echo sounder in a cage." IOTC, WPTT-22 4.

Quinn, T. J. and R. B. Deriso (1999). Quantitative fish dynamics, oxford university Press.

Santiago, J., J. Uranga, et al. (2019). A Novel Index of Abundance of Juvenile Yellowfin Tuna in the Indian Ocean Derived from Echosounder Buoys, IOTC–2019–WPTT21–47.

Santiago, J., J. Uranga, et al. (2020a). A novel index of abundance of skipjack in the Indian ocean derived from echosounder buoys, IOTC-2020-WPTT22(DP)-14.

Santiago, J., J. Uranga, et al. (2020b). "A novel index of abundance of juvenile yellowfin tuna in the Atlantic Ocean derived from echosounder buoys." Collect. Vol. Sci. Pap. ICCAT 76(6): 321-343.

Santiago, J., J. Uranga, et al. (2021). " Index of abundance of juvenile bigeye tuna in the Atlantic Ocean derived from echosounder buoys (2010-2020)." Collect. Vol. Sci. Pap. ICCAT, 78(2): 231-252.

Scott, G. P., & Lopez, J. (2014). The use of FADs in Tuna Fisheries. European Parliament. Policy Department B: Structural and Cohesion Policies: Fisheries. IP/B/PECH/IC/2013.

Simmons, E. and D. MacLennan (2005). "Fisheries acoustics." Theory and Practice. Second edition published by Blackwell Science.

Team, R. C. (2013). R: A language and environment for statistical computing.

Torres-Irineo, E., D. Gaertner, et al. (2014). "Changes in fishing power and fishing strategies driven by new technologies: The case of tropical tuna purse seiners in the eastern Atlantic Ocean." Fisheries Research 155: 10-19.

Wain, G., Guéry, L., Kaplan, D. M., & Gaertner, D. (2021). "Quantifying the increase in fishing efficiency due to the use of drifting FADs equipped with echosounders in tropical tuna purse seine fisheries." ICES Journal of Marine Science 78(1), 235-245.

Wessel, P., and W. H. F. Smith (1996). " A global, self-consistent, hierarchical, high-resolution shoreline database." J. Geophys. Res 101(B4), 8741-8743.

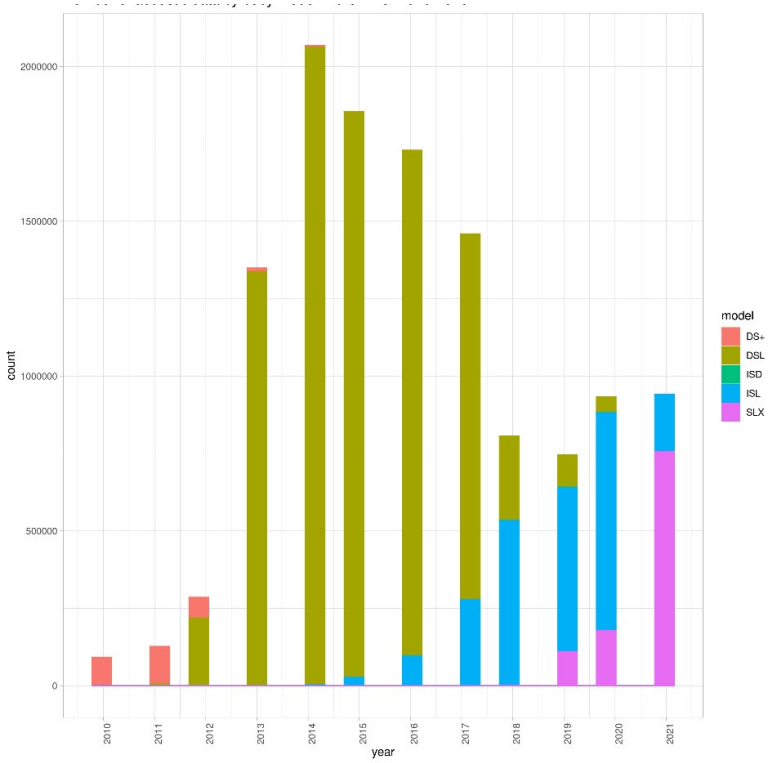

FIGURE 1. Buoy data distribution per model in the Pacific Ocean (2010-2021).
FIGURA 1. Distribución de datos de boyas por modelo en el Océano Pacífico (2010-2021).

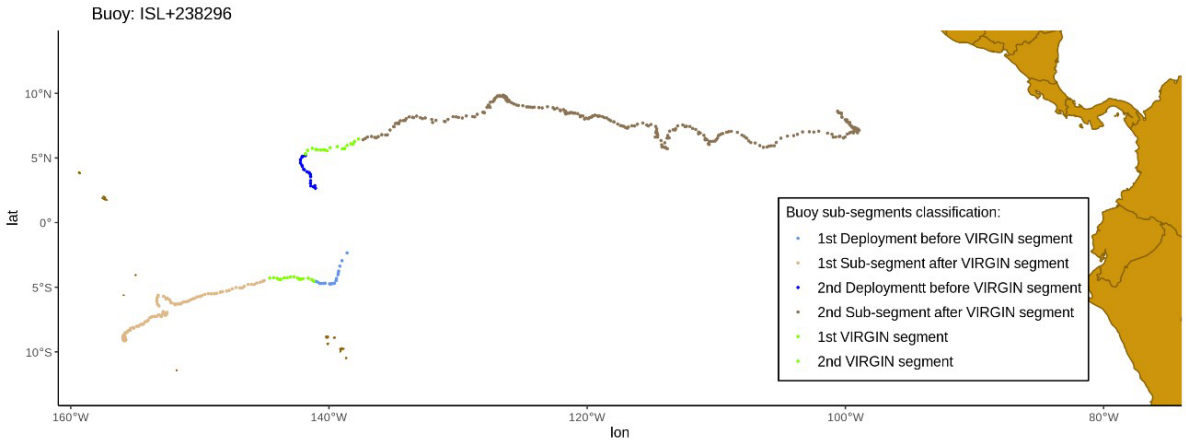

FIGURE 2. Example of "virgin" segments used for the calculation of the BAI index. Trajectories correspond to buoy ISL+284966 with two different paths representing drifts of different FADs. A virgin segment is defined as the segment of a buoy trajectory whose associated FAD likely represents a new deployment, which has been potentially colonized by tuna and not already fished. We consider as virgin segments (i.e. when tuna has aggregated to FAD) those segments of trajectories from 20-35 days at sea. "Virgin" segments are shown in green.
FIGURA 2. Ejemplo de segmentos "vírgenes" utilizados para el cálculo del índice IAB. Las trayectorias corresponden a la boya ISL+284966 con dos rutas distintas que representan derivas de diferentes plantados. Un segmento virgen se define como el segmento de la trayectoria de una boya cuyo plantado asociado probablemente representa una nueva siembra, que ha sido potencialmente colonizado por atunes y que aún no se ha pescado. Consideramos como segmentos vírgenes (es decir, cuando el atún se ha agregado a un plantado) aquellos segmentos de trayectorias de 20 a 35 días en el mar. Los segmentos "vírgenes" se muestran en verde.

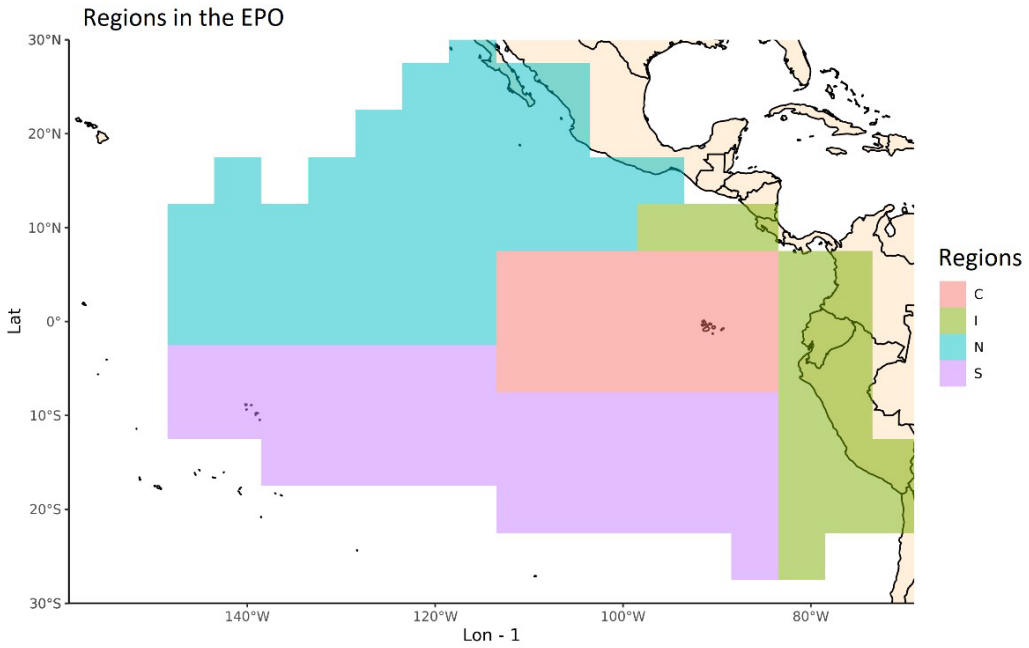

FIGURE 3. Length-frequency sampling areas defined by the IATTC staff for analyses of tropical tuna catches associated with floating objects.
FIGURA 3. Áreas de muestreo de frecuencia de tallas definidas por el personal de la CIAT para análisis de capturas de atunes tropicales asociadas con objetos flotantes.

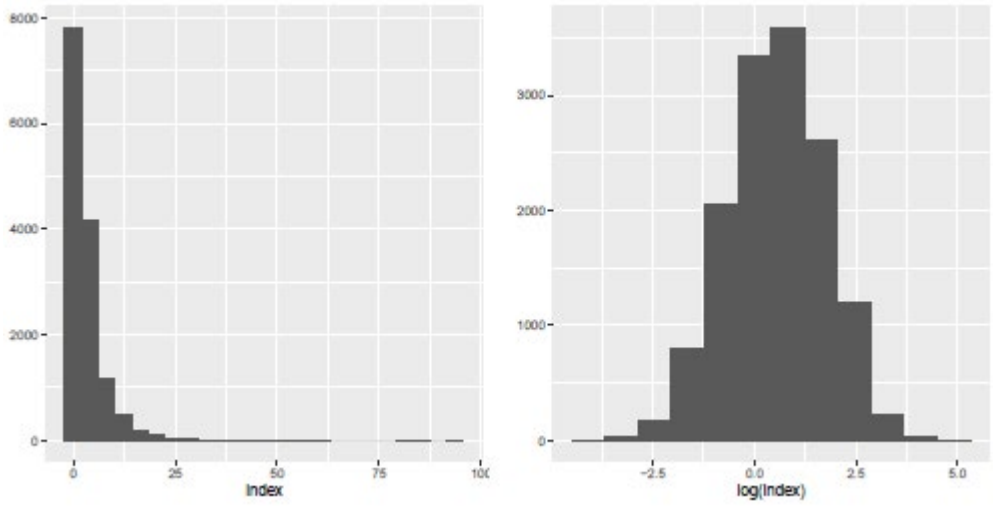

FIGURE 4. Histograms of the nominal values (left) and the log transformed nominal values (right) of the Buoy-derived Abundance Index (0.9 quantile of the integrated acoustic energy observations in "virgin" sequences).
FIGURA 4. Histogramas de los valores nominales (izquierda) y los valores nominales transformados logarítmicamente (derecha) del Índice de Abundancia Derivado de Boyas (cuantil de 0.9 de las observaciones de energía acústica integrada en secuencias "vírgenes").

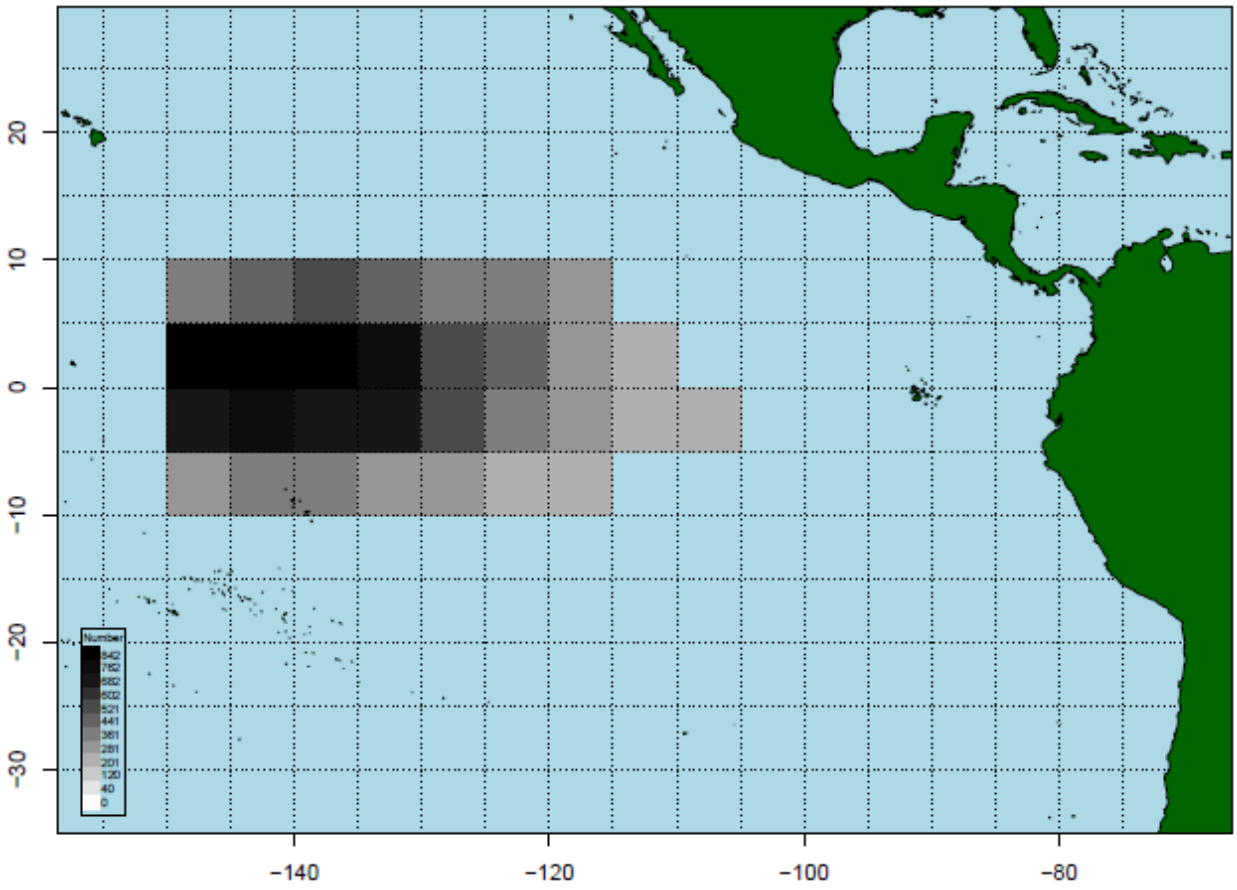

FIGURE 5. Spatial distribution [5°x5°] of the "virgin" sequences of buoy trajectories that have been used in the GLM analysis.

FIGURA 5. Distribución espacial [5°x5°] de las secuencias "vírgenes" de trayectorias de boyas que se han utilizado en el análisis MLG.

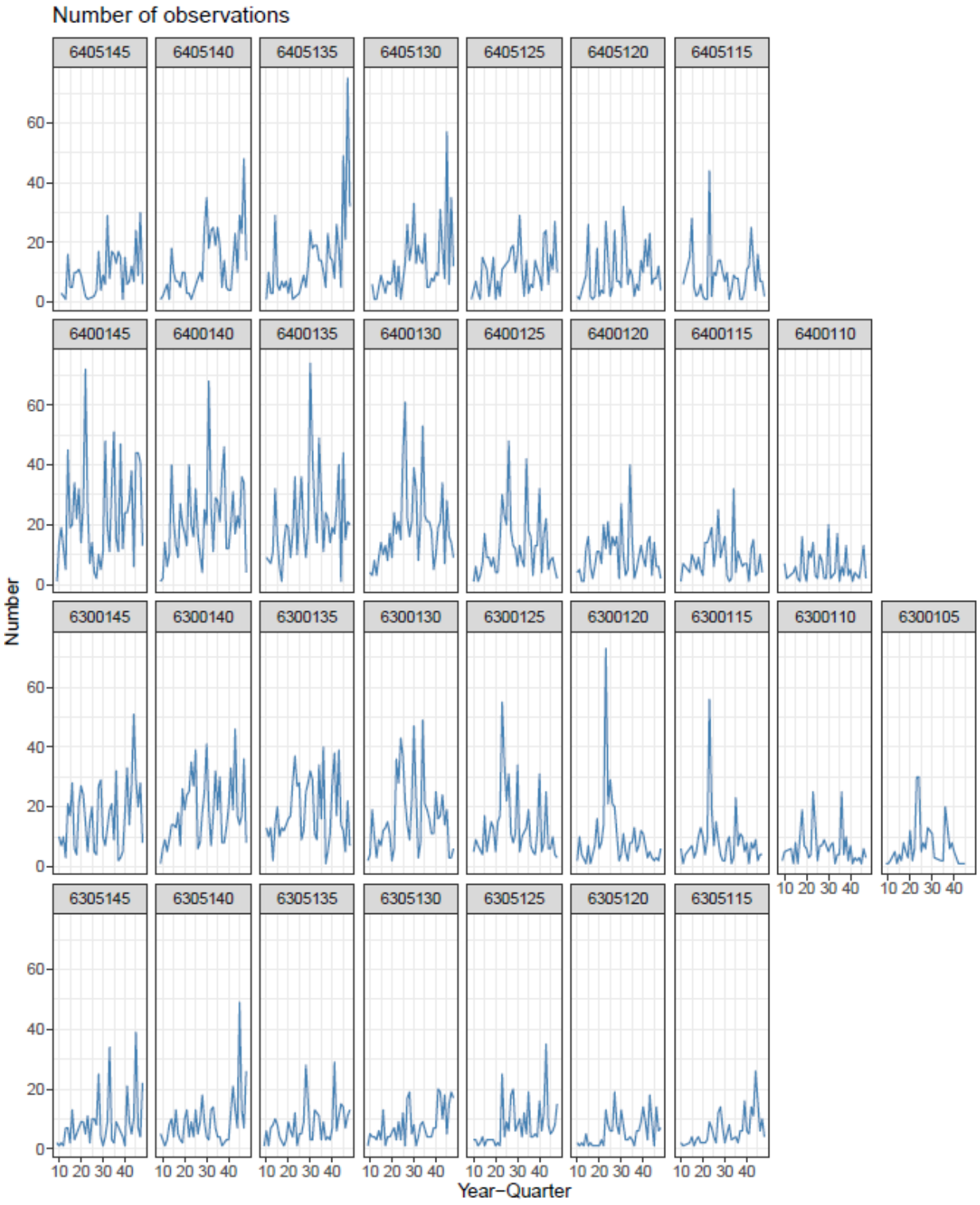

FIGURE 6. Quarterly evolution of the number of observations ("virgin" sequences of buoy trajectories) on a 5°x5° grid from 2012 to 2021.

FIGURA 6. Evolución trimestral del número de observaciones (secuencias "vírgenes" de trayectorias de boyas) en una cuadrícula de 5°x5° de 2012 a 2021.

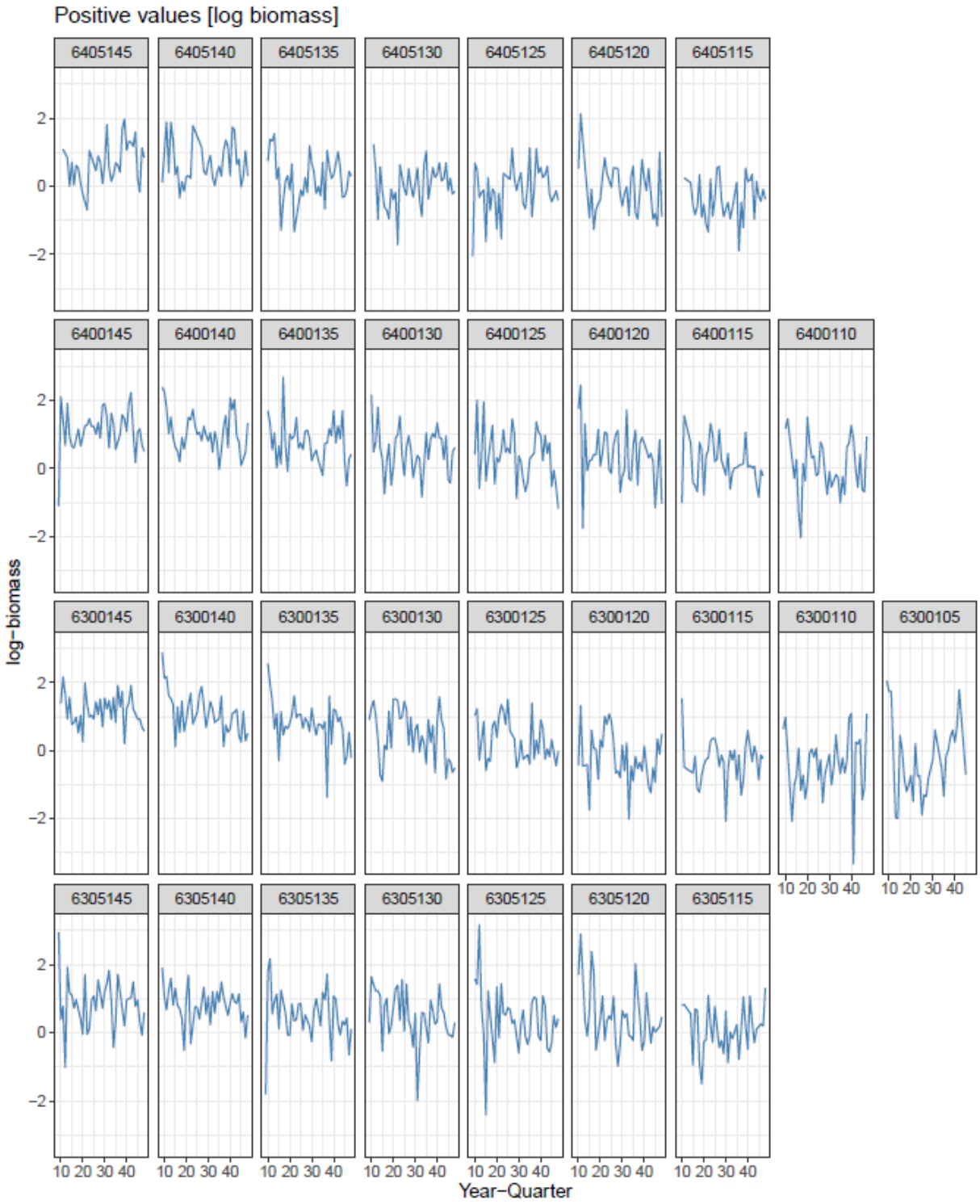

FIGURE 7. Quarterly evolution of the nominal log BAI index in the Atlantic Ocean by squares of 5x5 degrees from 2012 to 2021.

FIGURA 7. Evolución trimestral del índice IAB logarítmico nominal en el Océano Atlántico por cuadrados de 5x5 grados de 2012 a 2021.

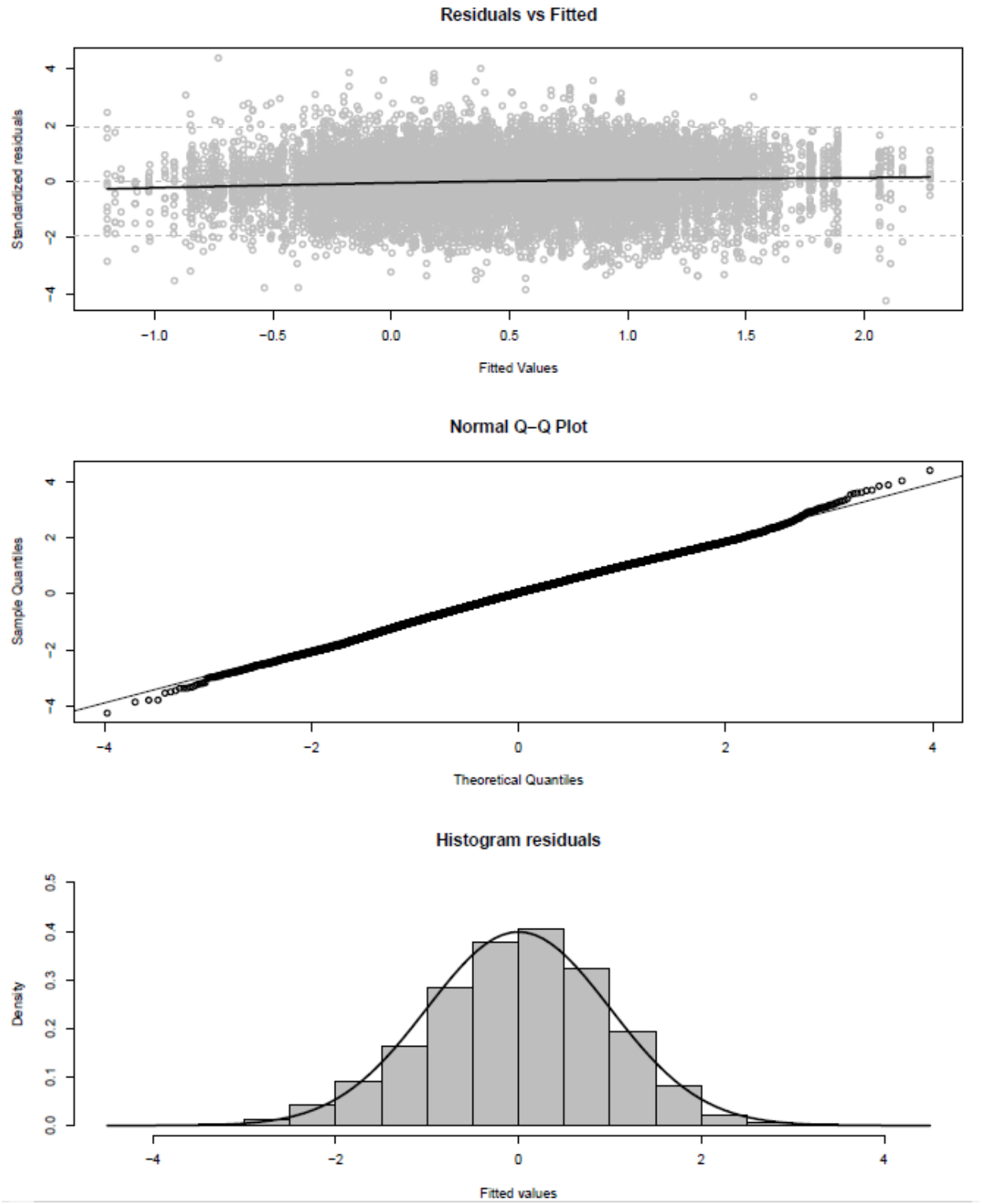

FIGURE 8. Diagnostics of the lognormal model selected for the period 2012-2020: residuals vs fitted, Normal Q-Q plot and frequency distributions of the residuals.
FIGURA 8. Diagnóstico del modelo lognormal seleccionado para el periodo 2012-2020: residuales vs. ajustados, gráfico Q-Q normal y distribuciones de frecuencia de los residuales.

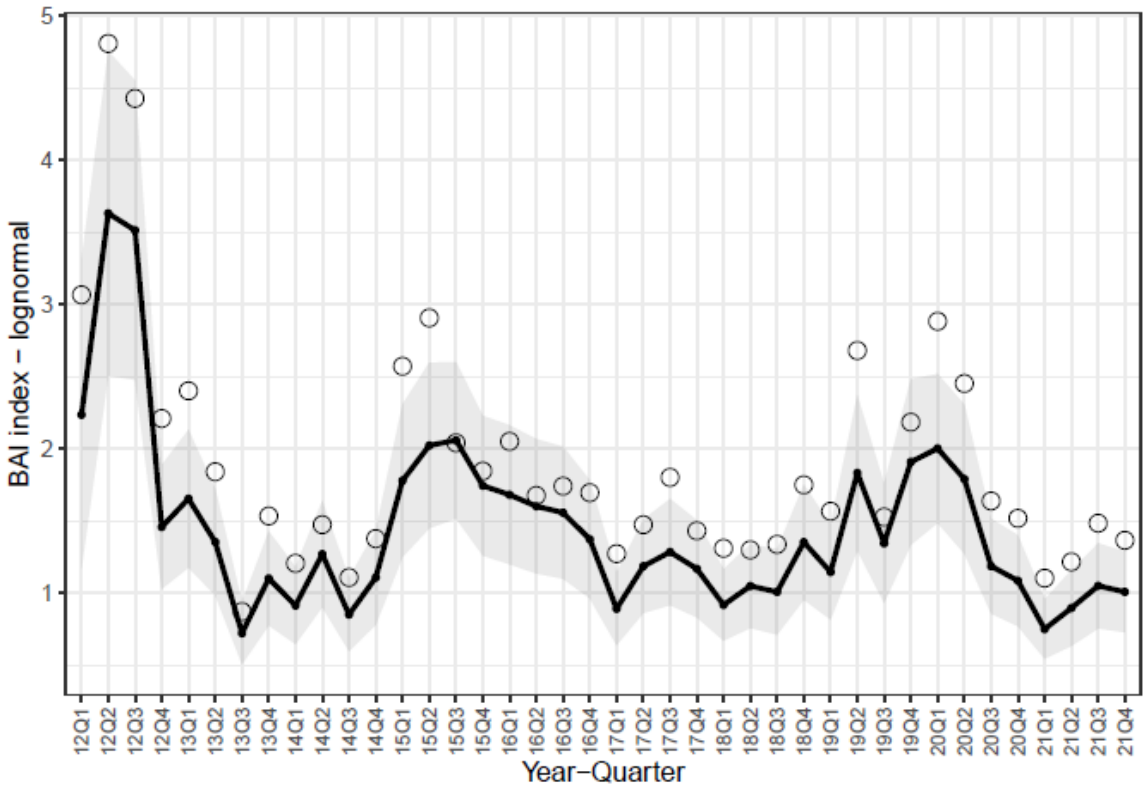

FIGURE 9. Time series of nominal (circles) and standardized (continuous line) Buoy-derived Abundance Index for the period 2012-2021. The 95% upper and lower confidence intervals of the standardized BAI index are shown by the grey shaded area.

FIGURA 9. Serie de tiempo del Índice de Abundancia Derivado de Boyas nominal (círculos) y estandarizado (línea continua) para el período 2012-2021. Los intervalos de confianza superior e inferior del 95% del índice IAB estandarizado se muestran en el área sombreada en gris.

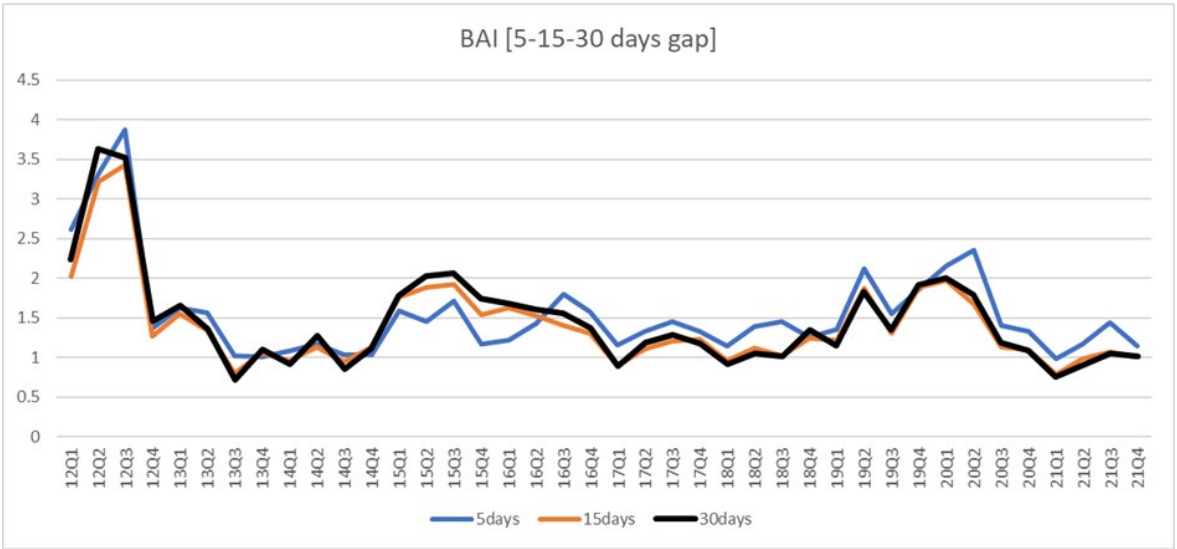

FIGURE 10. Time series of the standardized BAI index assuming thresholds of 5, 15 and 30 days between two consecutive observations of the same buoy. The threshold is used to identify trajectories of different FADs using the same buoy.

FIGURA 10. Serie de tiempo del índice IAB estandarizado suponiendo umbrales de 5, 15 y 30 días entre dos observaciones consecutivas de la misma boya. El umbral se utiliza para identificar trayectorias de diferentes plantados utilizando la misma boya.

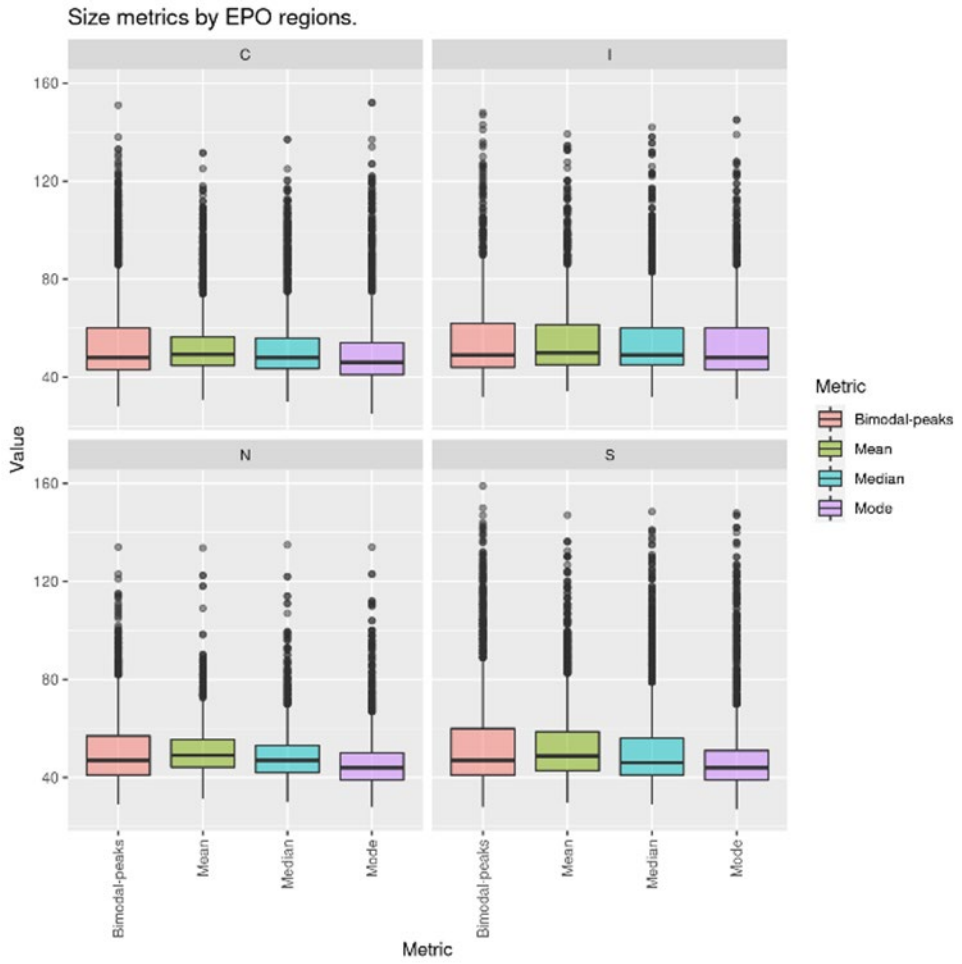

FIGURE 11. Distribution of sizes extracted by different metrics across the different regions of the EPO.
FIGURA 11. Distribución de tallas extraídas por diferentes medidas en las distintas regiones del OPO.

a)

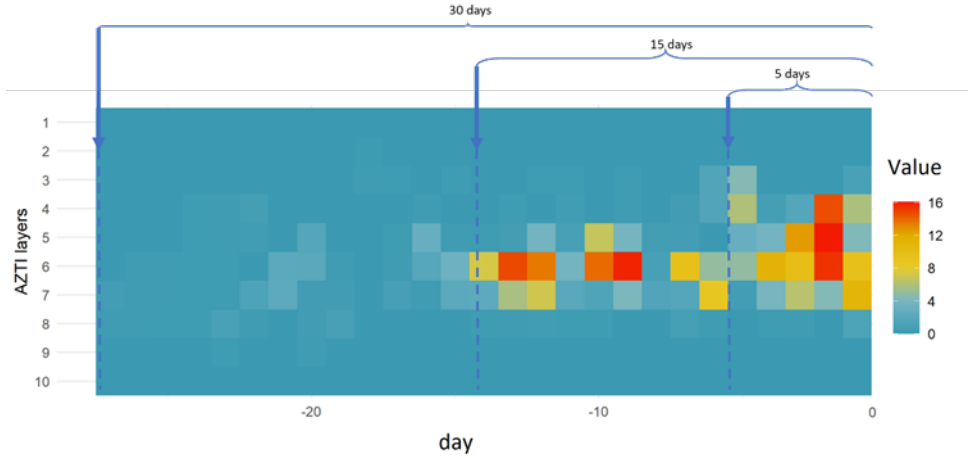

b)

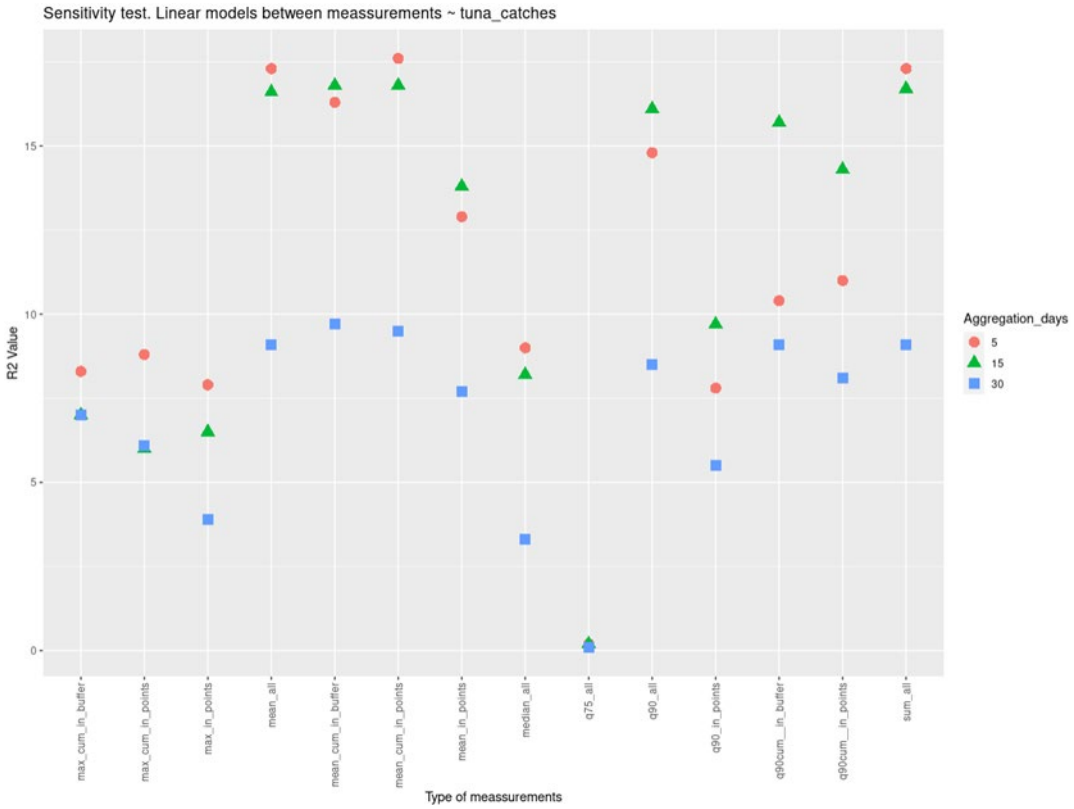

FIGURE 12. (a) Example of an echogram corresponding to a FAD before being fished, showing the three temporal windows explored in the analysis; (b) coefficient of determination of the linear regression between tuna catches by set and acoustic buoy biomass estimates for the sensitivity test with different combinations of time frame and parameters used to select the variables of the linear regression.

FIGURA 12. (a) Ejemplo de un ecograma correspondiente a un plantado antes de ser pescado, que muestra las tres ventanas temporales exploradas en el análisis; (b) coeficiente de determinación de la regresión lineal entre las capturas de atunes por lance y las estimaciones de biomasa de boya acústica para la prueba de sensibilidad con diferentes combinaciones de marco temporal y parámetros utilizados para seleccionar las variables de la regresión lineal.

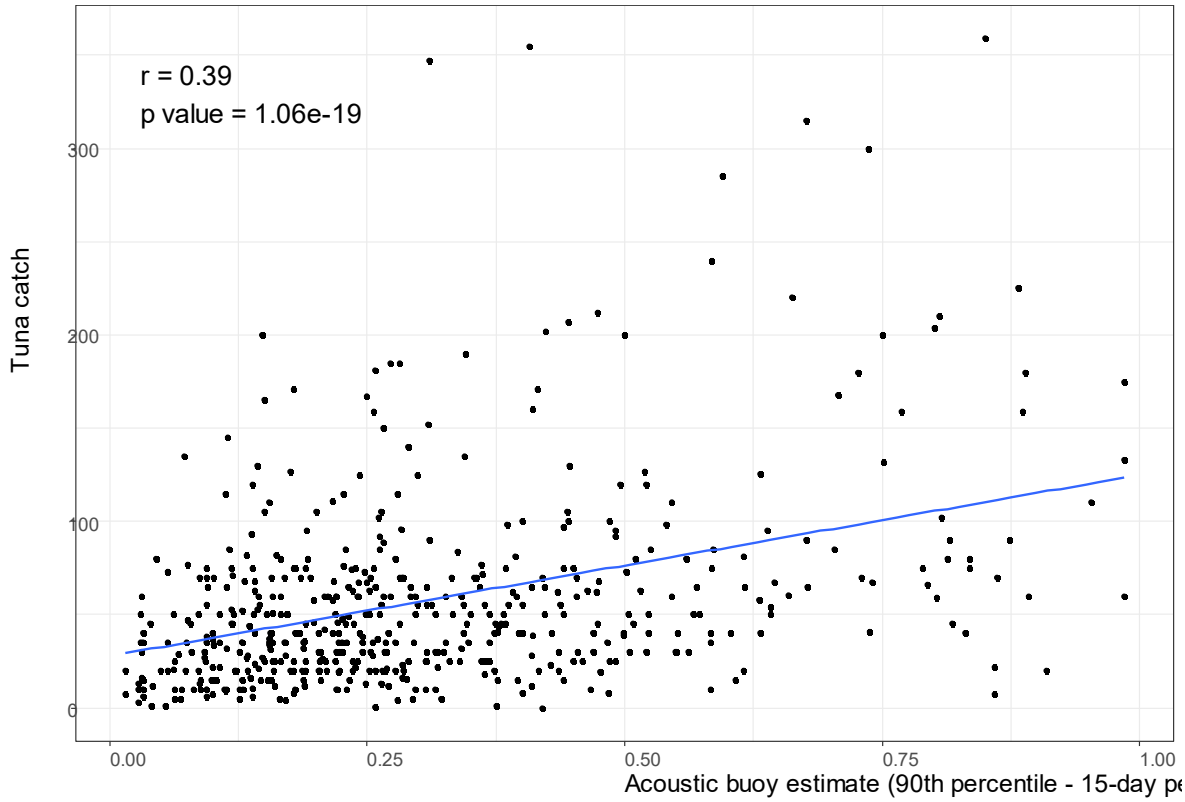

FIGURE 13. Scatter diagram and linear regression of tuna catches by set against acoustic buoy biomass estimates (90th quantile of a 15-day window prior to the set). [EPO observer data, 2019-2021].
FIGURA 13. Diagrama de dispersión y regresión lineal de las capturas de atunes por lance frente a estimaciones de biomasa de boyas acústicas (cuantil de 90 de una ventana de 15 días antes del lance). [Datos de observadores del OPO, 2019-2021]

TABLE 1. Technical specifications of different buoy models and observed values over analysis data.
TABLA 1. Especificaciones técnicas de diferentes modelos de boyas y valores observados sobre datos de análisis.

Model	Typical setup						Mean observed values over analysis data	
	Beam angle	Sounder frequency	Power	Frequency of acoustic sampling (ping rate)	Daily acoustic data recorded	Frequency of transmission	Number of buoys	Sampling frequency
DS+	32º	190.5 kHz	100 W	3	3	24h	1428	1.36
DSL+	32º	190.5 kHz	100 W	3	3	24h	12462	2.82
ISL+	32º	190.5 kHz	100 W	15 min	variable (reset at dusk)	24h	23	1.67
ISD+	32º	200/38 kHz (38 kHz not provided)	100 W	15 min	variable (reset at dusk)	24h	6214	1.21
SLX+	32º	200	100 W	5 min	variable (Sunrise or Alarms based)	24h	785	1.98

TABLE 2. Deviance table for the GLM lognormal model of the 2012-2021 period.
TABLA 2. Tabla de desviación del modelo lognormal MLG del período 2012-2021.

Variable	Df	Deviance	Resid..Df	Resid..Dev	F	Pr..F.	Dev..Exp
NULL	NA	NA	13867	19453	NA	NA	NA
yyqq	39	1363	13828	18089	36	0.0000	7.01%
area	30	2527	13798	15562	86	0.0000	12.99%
model	2	78	13796	15484	40	0.0000	0.4%
den	1	88	13795	15396	90	0.0000	0.45%
chl	1	9	13794	15387	9	0.0022	0.05%
sst	1	11	13793	15376	11	0.0009	0.06%
mld	1	97	13792	15278	99	0.0000	0.5%
yyqq:area	1086	2569	12706	12709	2	0.0000	13.21%
yyqq:model	34	123	12672	12586	4	0.0000	0.63%
yyqq:den	38	103	12634	12483	3	0.0000	0.53%
yyqq:sst	39	101	12595	12382	3	0.0000	0.52%
yyqq:mld	39	73	12556	12309	2	0.0006	0.37%

TABLE 3. Nominal and standardized Buoy-derived Abundance Index for the period 2012-2021. Standard errors and coefficient of variations of the standardized series are also included.
TABLA 3. Índice de Abundancia Derivado de las Boyas nominal y estandarizado para el período 2012-2021. También se incluyen los errores estándar y el coeficiente de variación de la serie estandarizada.

Quarter	Index nominal	BAI index	BAI se	BAI cv
12Q1	3.069	2.238	0.544	0.243
12Q2	4.812	3.634	0.573	0.158
12Q3	4.431	3.517	0.530	0.151
12Q4	2.213	1.460	0.219	0.150
13Q1	2.404	1.657	0.243	0.147
13Q2	1.843	1.356	0.188	0.139
13Q3	0.874	0.724	0.109	0.151
13Q4	1.537	1.104	0.166	0.150
14Q1	1.209	0.916	0.136	0.149
14Q2	1.476	1.272	0.187	0.147
14Q3	1.110	0.853	0.129	0.151
14Q4	1.380	1.110	0.167	0.150
15Q1	2.575	1.782	0.270	0.151
15Q2	2.910	2.025	0.293	0.145
15Q3	2.043	2.062	0.277	0.134
15Q4	1.848	1.747	0.247	0.141
16Q1	2.054	1.684	0.246	0.146
16Q2	1.679	1.604	0.238	0.148
16Q3	1.744	1.560	0.234	0.150
16Q4	1.698	1.375	0.209	0.152
17Q1	1.275	0.893	0.128	0.143
17Q2	1.476	1.188	0.166	0.139
17Q3	1.804	1.287	0.188	0.146
17Q4	1.434	1.171	0.172	0.147
18Q1	1.313	0.920	0.126	0.137
18Q2	1.302	1.051	0.148	0.141
18Q3	1.340	1.010	0.151	0.150
18Q4	1.752	1.355	0.203	0.150
19Q1	1.569	1.148	0.168	0.146
19Q2	2.683	1.835	0.274	0.149
19Q3	1.529	1.347	0.210	0.156
19Q4	2.187	1.911	0.293	0.153
20Q1	2.886	2.005	0.263	0.131
20Q2	2.455	1.793	0.263	0.147
20Q3	1.641	1.189	0.168	0.141
20Q4	1.520	1.088	0.161	0.148
21Q1	1.106	0.753	0.105	0.139
21Q2	1.219	0.899	0.134	0.149
21Q3	1.487	1.052	0.151	0.143
21Q4	1.368	1.010	0.143	0.141